Radiative Transfer in Water Clouds in the 10-Micron Window Region[1]

GIICHI YAMAMOTO, MASAYUKI TANAKA AND KAZUO KAMITANI

Geophysical Institute, Tohoku University, Sendai, Japan

(Manuscript received 17 January 1966)

ABSTRACT

The equation of radiative transfer as applied to water clouds in the window region near 10 microns is solved numerically by using values of the phase function and albedo for single scattering estimated by Deirmendjian (1964). It is found that for monochromatic radiation of 10 microns the upward intensity at the cloud top shows limb darkening and the downward intensity at the cloud base, limb brightening. For the whole window region from 8 to 12 microns, the upward flux at the cloud top and the downward flux at the cloud base, as well as the emissivity of the cloud, transmissivity at the cloud top and reflectivity at the cloud base are evaluated. When the cloud is thin, the upward flux is mostly dependent on the incident flux corresponding to the earth surface temperature, and when the cloud becomes thick, it approaches the blackbody flux at the cloud temperature. The downward flux at the cloud base is very small for a thin cloud, increases with cloud thickness and approaches a constant value which is somewhat larger than the upward flux at the cloud top when the cloud becomes very thick. It is also found that the emissivity, transmissivity and reflectivity change with cloud thickness but are practically independent of both the cloud and earth surface temperatures. Therefore, by using the values of these quantities obtained in this study, one can evaluate the upward and downward fluxes for any combination of cloud and earth surface temperatures and cloud thicknesses.

1. Introduction

In problems of atmospheric radiative transfer, it is generally assumed that clouds are perfect black bodies. In the case of a thin cloud such as cirrus, however, this assumption is abandoned by many workers, and it is sometimes assumed that the emissivity of cirrus is about 0.5. This assumption, of course, is not based on firm ground, and is used only for the purpose of obtaining numerical results. Essentially the emissivity of a thin cloud depends upon the thickness and temperature of the cloud, the size distribution of cloud droplets, and whether they are water droplets or ice crystals. In order to evaluate the emissivity of a cloud, or more generally, the radiative characteristics of the cloud, it is necessary to solve the equation of radiative transfer as applied to the cloud. In the infrared region, because the size of cloud droplets is of the same order as the wavelength of radiation, we need to take into account the scattering process as well as the process of emission and absorption.

In this investigation we shall consider the window region, taking the wavelength of 10 microns as representative, because the effect of imperfect blackness of a thin cloud is most predominant in this region. Then, the equation of radiative transfer will be solved numerically for model clouds whose drop-size distribution is given by Deirmendjian (1964).

[1] This work was supported by the Environmental Science Services Administration under Contract No. Cwb-11186.

2. Optical properties of clouds

The complex refractive index of water in the infrared region has been compiled by Dorsey (1940) and Centeno (1941) based on earlier works. Later Plyler and Acquista (1954) measured the absorptivity of water in the spectral region between 2 and 42 microns, and McDonald (1960) calculated the imaginary part of the refractive index of water based on Plyler and Acquista's measurements. His values are about half of those of Centeno's in the wavelength region from 6 to 10 microns, and he cites some evidence in support of his results. Herman (1962) then evaluated the efficiency factor of the Mie scattering for water droplets using Dorsey's values for the real part and McDonald's values for the imaginary part of the refractive index of water. Deirmendjian (1964) recently calculated the phase function for cloud droplets at several wavelengths in the infrared region based on Centeno's values of the complex refractive index.

It seems, therefore, that there is room for discussion of Deirmendjian's results with regard to his choice of the basic data. However, at present, we have not yet sufficiently strong evidence to reject Centeno's values, and it furthermore seems unlikely that there would be much difference from Deirmendjian's results, even if Plyler and Acquista's values were used. Therefore, in this investigation we shall use the phase function estimated by Deirmendjian for a model cloud whose drop-size distribution is given by

$$n(r)\sim r^6 e^{-1.5r}, \tag{1}$$

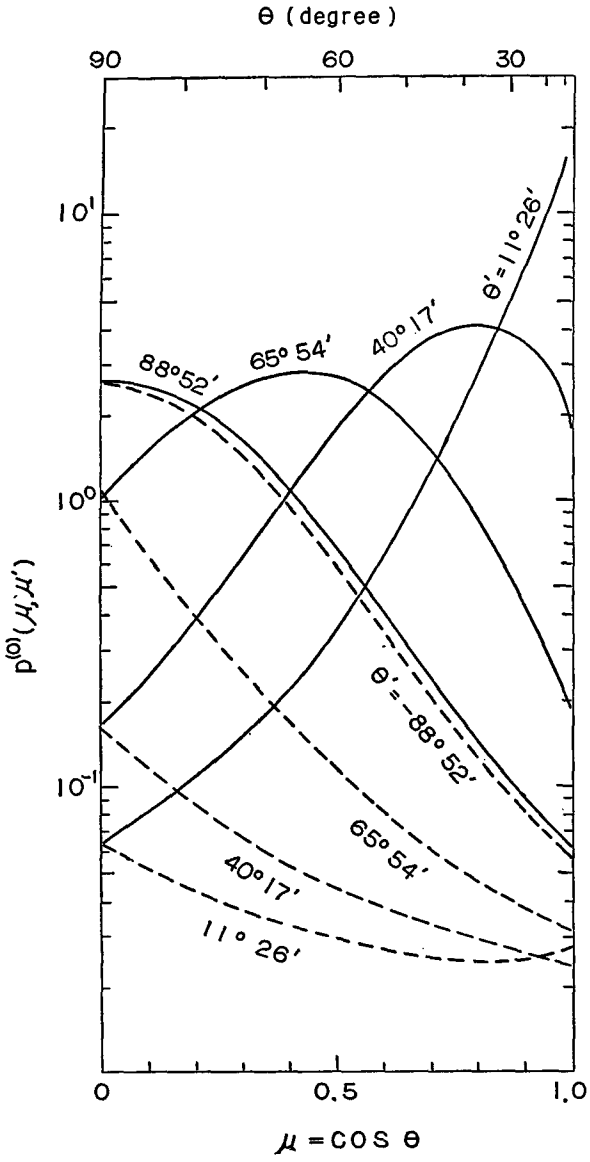

FIG. 1. Phase function $p^{(0)}(\mu,\mu')$ for cloud droplets at $\lambda=10$ microns. Solid lines correspond to the forward scattering, and broken lines to the backward scattering.

where $n(r)$ is the volume concentration at the radius r. He calculated the phase function $p(\mu, \varphi; \mu', \varphi')$, where μ represents the cosine of the polar angle and φ the azimuthal angle, respectively, of the scattered radiation, and μ' and φ' represent similar quantities of the incident radiation.

In this investigation the cloud is assumed to be isothermal and homogeneous. In addition, as we are considering the window region where the intensity of solar radiation is negligible, the radiation field can reasonably be assumed to be independent of the azimuthal angle. Then the phase function $p^{(0)}(\mu,\mu')$ defined by

$$p^{(0)}(\mu,\mu')=\frac{1}{2\pi}\int_0^{2\pi} p(\mu, \varphi; \mu', \varphi')d\varphi', \qquad (2)$$

is necessary and is accordingly calculated from Deirmendjian's result. Fig. 1 shows the values of $p^{(0)}(\mu,\mu')$ for cloud droplets at a wavelength of 10 microns as a function of μ or θ, taking θ' as a parameter. In the figure the solid and broken lines correspond to the phase function of the forward and backward scattering respectively. The predominancy of the forward scattering which is the characteristic property of Mie scattering is clearly exhibited in the figure.

The albedo for single scattering, ω, which is defined as the ratio of the volume scattering coefficient to the volume extinction (i.e., scattering plus absorption) coefficient, is also a characteristic quantity representing an optical property of the cloud. As described above there is some question as to Deirmendjian's values of ω. However, in order to be consistent with his phase function, Deirmendjian's value is used in calculating the intensity of 10 micron radiation. In the calculation of radiation flux in the whole window region from 8 to 12 microns, we have assumed the same phase function as calculated for 10 microns. Of course the phase function

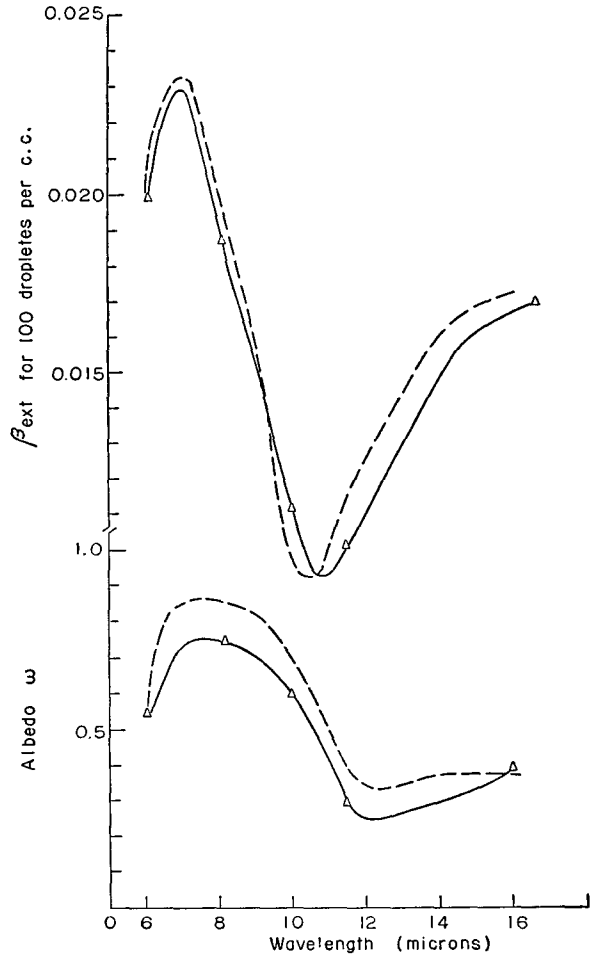

FIG. 2. Albedo ω and volume extinction coefficients β_{ext} as a function of wavelength. Solid lines are drawn based on Deirmendjian's computations, and broken lines, on Herman's efficiency factor.

differs with wavelength. However, the phase function to be used in this study is already averaged over φ, and normalized to one when averaged over μ and φ, so that it is unlikely that a small change of the present phase function with wavelength would cause a large change in the calculation. However, the change of ω with wavelength is taken into account. This is because ω is very sensitive to the intensity of radiation, and thus to the flux, as can be inferred from the equation of radiative transfer which will appear later. Since Deirmendjian's calculation of ω does not cover the window region closely, we have made some supplementary calculations based on Centeno's values of the complex refractive index. Fig. 2 shows the values of ω and corresponding extinction coefficient, β_{ext}, as a function of wavelength. In the figure the values of ω and β_{ext} based on Herman's efficiency factor are also shown as a reference.

In considering radiative transfer in the window region, the effect of water vapor which exists in the cloud is not as important compared to that of cloud droplets, so that it is neglected in this study. The effect of water vapor, which exists in the atmosphere between the cloud and earth surface, is also small in the window region. However, it will make the incident radiation at the cloud base anisotropic, i.e., dependent on the angle of incidence, so that it is taken into account in some cases. The transmission values of water vapor in the window region derived by Wark *et al.* (1962) are used for this calculation.

3. Theory

We consider a plane-parallel atmosphere which has a cloud layer above and a cloudless dry or moist layer below. The optical thickness from the top of the cloud to a layer in the cloud is denoted by τ and the total optical thickness of the cloud is given by τ_1. The radiation field in the cloud is then expressed by the following equation of radiative transfer:

$$\mu\frac{dI_\nu(\tau;\mu)}{d\tau}=I_\nu(\tau;\mu)-\frac{\omega}{2}\int_{-1}^{+1}p^{(0)}(\mu,\mu')I_\nu(\tau;\mu')d\mu'-(1-\omega)B_\nu(T_c), \quad (3)$$

where I_ν is the intensity of radiation for frequency ν, and $B_\nu(T_c)$ is the Plank function for the cloud temperature T_c. From the assumptions that no incident radiation exists at the cloud top and that the incident radiation at the cloud base is independent of the azimuthal angle, i.e., axially symmetric at every point, the boundary conditions for I_ν are given by

$$\left.\begin{aligned} I_\nu(0;\ -\mu)&=0\\ I_\nu(\tau_1;\ +\mu)&=f(\mu)\end{aligned}\right\}, \quad (4)$$

where $f(\mu)$ is determined from the surface temperature, and the temperature, pressure, and water vapor distributions in the atmosphere below the cloud.

In solving (3) under the conditions (4), we shall separate the radiation field in the cloud into two parts; i) that due to the external field and ii) that due to the emission in the cloud. Let the intensity of i) be $I_{\nu,s}$ and that of ii), $I_{\nu,e}$. Then we have

$$I_\nu=I_{\nu,s}+I_{\nu,e}. \quad (5)$$

The equation for $I_{\nu,s}$ lacks the last term of (3), so that it is given by

$$\mu\frac{dI_{\nu,s}(\tau;\mu)}{d\tau}=I_{\nu,s}(\tau;\mu)-\frac{\omega}{2}\int_{-1}^{+1}p^{(0)}(\mu,\mu')I_{\nu,s}(\tau;\mu')d\mu', \quad (6)$$

and

$$\left.\begin{aligned} I_{\nu,s}(0;\ -\mu)&=0\\ I_{\nu,s}(\tau_1;\ +\mu)&=f(\mu)\end{aligned}\right\}. \quad (7)$$

The equation for $I_{\nu,e}$ is

$$\mu\frac{dI_{\nu,e}(\tau;\mu)}{d\tau}=I_{\nu,e}(\tau;\mu)-\frac{\omega}{2}\int_{-1}^{+1}p^{(0)}(\mu,\mu')I_{\nu,e}(\tau;\mu')d\mu'-(1-\omega)B_\nu(T_c), \quad (8)$$

with the boundary conditions

$$\left.\begin{aligned} I_{\nu,e}(0;\ -\mu)&=0\\ I_{\nu,e}(\tau_1;\ +\mu)&=0\end{aligned}\right\}. \quad (9)$$

In this investigation the quantities in which we are mostly interested are $I_\nu(0;+\mu)$, the upward intensity at the cloud top, and $I_\nu(\tau_1;-\mu)$, the downward intensity at the cloud base. Then the solution of (6) can be expressed by using the transmission and scattering functions T and S, respectively, which have been introduced by Chandrasekhar (1950), as follows:

$$I_{\nu,s}(0;+\mu)=f(\mu)e^{-\tau_1/\mu}+\frac{1}{2\mu}\int_0^1 f(\mu')T(\tau_1;\mu,\mu')d\mu', \quad (10)$$

and

$$I_{\nu,s}(\tau_1;-\mu)=\frac{1}{2\mu}\int_0^1 f(\mu')S(\tau_1;\mu,\mu')d\mu', \quad (11)$$

where T and S apply to the azimuthally independent case and are defined as the solution of the following integral equations:

$$\left(\frac{1}{\mu}-\frac{1}{\mu'}\right)T(\tau_1;\mu,\mu')=\omega p^{(0)}(-\mu,-\mu')(e^{-\tau_1/\mu'}-e^{-\tau_1/\mu})$$
$$+\frac{\omega}{2}\int_0^1 p^{(0)}(-\mu,-\mu'')T(\tau_1;\mu'',\mu')\frac{d\mu''}{\mu''}-\frac{\omega}{2}\int_0^1 T(\tau_1;\mu,\mu'')p^{(0)}(-\mu'',-\mu')\frac{d\mu''}{\mu''}$$
$$+\frac{\omega}{2}e^{-\tau_1/\mu'}\int_0^1 S(\tau_1;\mu,\mu'')p^{(0)}(\mu'',-\mu')\frac{d\mu''}{\mu''}-\frac{\omega}{2}e^{-\tau_1/\mu}\int_0^1 p^{(0)}(-\mu,\mu'')S(\tau_1;\mu'',\mu')\frac{d\mu''}{\mu''}$$
$$+\frac{\omega}{4}\int_0^1\int_0^1 S(\tau_1;\mu,\mu'')p^{(0)}(\mu'',-\mu''')T(\tau_1;\mu''',\mu')\frac{d\mu''}{\mu''}\frac{d\mu'''}{\mu'''}$$
$$-\frac{\omega}{4}\int_0^1\int_0^1 T(\tau_1;\mu,\mu'')p^{(0)}(-\mu'',\mu''')S(\tau_1;\mu''',\mu')\frac{d\mu''}{\mu''}\frac{d\mu'''}{\mu'''}, \quad (12)$$

$$\left(\frac{1}{\mu}+\frac{1}{\mu'}\right)S(\tau_1;\mu,\mu')=\omega p^{(0)}(\mu,-\mu')\left[1-\exp\left\{-\tau_1\left(\frac{1}{\mu}+\frac{1}{\mu'}\right)\right\}\right]$$
$$+\frac{\omega}{2}\int_0^1 p^{(0)}(\mu,\mu'')S(\tau_1;\mu'',\mu')\frac{d\mu''}{\mu''}+\frac{\omega}{2}\int_0^1 S(\tau_1;\mu,\mu'')p^{(0)}(-\mu'',-\mu')\frac{d\mu''}{\mu''}$$
$$-\frac{\omega}{2}e^{-\tau_1/\mu}\int_0^1 p^{(0)}(\mu,-\mu'')T(\tau_1;\mu'',\mu')\frac{d\mu''}{\mu''}-\frac{\omega}{2}e^{-\tau_1/\mu'}\int_0^1 T(\tau_1;\mu,\mu'')p^{(0)}(\mu'',-\mu')-\frac{d\mu''}{\mu''}$$
$$+\frac{\omega}{4}\int_0^1\int_0^1 S(\tau_1;\mu,\mu'')p^{(0)}(-\mu'',\mu''')S(\tau_1;\mu''',\mu')\frac{d\mu''}{\mu''}\frac{d\mu'''}{\mu'''}$$
$$-\frac{\omega}{4}\int_0^1\int_0^1 T(\tau_1;\mu,\mu'')p^{(0)}(\mu'',-\mu''')T(\tau_1;\mu''',\mu')\frac{d\mu''}{\mu''}\frac{d\mu'''}{\mu'''}. \quad (13)$$

The function $p^{(0)}(\mu,\mu')$ satisfies the symmetry relations given by,

$$p^{(0)}(\mu,\mu')=p^{(0)}(-\mu,-\mu'), \quad (14)$$

$$p^{(0)}(\mu,-\mu')=p^{(0)}(\mu',-\mu). \quad (15)$$

By use of (14) and (15) Helmholtz's principle of reciprocity, which should also be satisfied by the functions T and S, can be expressed as

$$T(\tau_1;\mu,\mu')=T(\tau_1;\mu',\mu), \quad (16)$$

$$S(\tau_1;\mu,\mu')=S(\tau_1;\mu',\mu). \quad (17)$$

Next, we shall consider $I_{\nu,e}$. As we have assumed that the cloud is homogeneous and isothermal, we have the relation,

$$I_{\nu,e}(0;+\mu)=I_{\nu,e}(\tau_1;-\mu)\equiv E_\nu(\tau_1;\mu), \quad (18)$$

where we shall introduce $E_\nu(\tau_1;\mu)$ as the emission function of the cloud. A similar relation holds for a part of the cloud with thickness τ, if the radiative interaction by the rest of the cloud is taken out of consideration. By use of the emission function, the mathematical expression of the principle of invariance, which is generally given by four equations, is reduced to the following two equations:

$$E_\nu(\tau_1;+\mu)=E_\nu(\tau;+\mu)+e^{-\tau/\mu}I_{\nu,e}(\tau;+\mu)$$
$$+\frac{1}{2\mu}\int_0^1 T(\tau;\mu,\mu')I_{\nu,e}(\tau;+\mu')d\mu', \quad (19)$$

$$I_{\nu,e}(\tau;+\mu)=E_\nu(\tau_1-\tau;+\mu)$$
$$+\frac{1}{2\mu}\int_0^1 S(\tau_1-\tau;\mu,\mu')I_{\nu,e}(\tau;-\mu')d\mu'. \quad (20)$$

Eliminating $I_{\nu,e}$ from (8), (9), (19) and (20), we have the integral equation for $E_\nu(\tau_1;\mu)$,

$$E(\tau_1;\mu)=(1-e^{-\tau_1/\mu})(1-\omega)B_\nu(T_c)+\frac{\omega}{2}\int_0^1 p^{(0)}(\mu,\mu')E(\tau_1;\mu')d\mu'$$

$$-\frac{\omega}{2}e^{-\tau_1/\mu}\int_0^1 p^{(0)}(\mu,-\mu')E(\tau_1;\mu')d\mu'+\tfrac{1}{2}(1-\omega)B_\nu(T_c)\int_0^1\{S(\tau_1;\mu,\mu')-T(\tau_1;\mu,\mu')\}\frac{d\mu'}{\mu'}$$

$$+\frac{\omega}{4}\int_0^1\{S(\tau_1;\mu,\mu')-T(\tau_1;\mu,\mu')\}\frac{d\mu'}{\mu'}\int_0^1 p^{(0)}(\mu',-\mu'')E(\tau_1;\mu'')d\mu''. \quad (21)$$

By solving the integral equations (12), (13) and (21) and using necessary relations shown above, we can evaluate the intensity of emergent radiations at the top and base of the cloud.

4. Process of numerical calculation

In order to evaluate T and S from (12) and (13), we shall follow the method of expanding them in a power series of ω, which has been applied by Goldstein (1960) and Gross (1962) for the problem of diffuse reflection in a semi-infinite atmosphere. Thus,

$$T(\tau_1;\mu,\mu')=\sum_n \omega^n T_n(\tau_1;\mu\ \mu'), \quad (22)$$

and

$$S(\tau_1;\mu,\mu')=\sum_n \omega^n S_n(\tau_1;\mu,\mu'). \quad (23)$$

Substituting (22) and (23) in (12) and (13), we have the recursion relations

$$T_0(\tau_1;\mu,\mu')=0,$$

$$\left(\frac{1}{\mu}-\frac{1}{\mu'}\right)T_1(\tau_1;\mu,\mu')=(e^{-\tau_1/\mu'}-e^{-\tau_1/\mu})p^{(0)}(-\mu,-\mu'),$$

$$\left(\frac{1}{\mu}-\frac{1}{\mu'}\right)T_2(\tau_1;\mu,\mu')=\frac{1}{2}\int_0^1 p^{(0)}(-\mu,-\mu'')T_1(\tau_1;\mu'',\mu')\frac{d\mu''}{\mu''}$$

$$-\frac{1}{2}\int_0^1 T_1(\tau_1;\mu,\mu'')p^{(0)}(-\mu'',-\mu')\frac{d\mu''}{\mu''}+\tfrac{1}{2}e^{-\tau_1/\mu'}\int_0^1 S_1(\tau_1;\mu,\mu'')p^{(0)}(\mu'',-\mu')\frac{d\mu''}{\mu''}$$

$$-\tfrac{1}{2}e^{-\tau_1/\mu}\int_0^1 p^{(0)}(-\mu,\mu'')S_1(\tau_1;\mu'',\mu')\frac{d\mu''}{\mu''}, \quad (24)$$

etc.

Similarly,

$$S_0(\tau_1;\mu,\mu')=0,$$

$$\left(\frac{1}{\mu}+\frac{1}{\mu'}\right)S_1(\tau_1;\mu,\mu')=\left[1-\exp\left\{-\tau_1\left(\frac{1}{\mu}+\frac{1}{\mu'}\right)\right\}\right]p^{(0)}(\mu,-\mu'),$$

$$\left(\frac{1}{\mu}+\frac{1}{\mu'}\right)S_2(\tau_1;\mu,\mu')=\frac{1}{2}\int_0^1 p^{(0)}(\mu,\mu'')S_1(\tau_1;\mu'',\mu')\frac{d\mu''}{\mu''}$$

$$+\frac{1}{2}\int_0^1 S_1(\tau_1;\mu,\mu'')p^{(0)}(-\mu'',-\mu')\frac{d\mu''}{\mu''}-\tfrac{1}{2}e^{-\tau_1/\mu}\int_0^1 p^{(0)}(\mu,-\mu'')T_1(\tau_1;\mu'',\mu')\frac{d\mu''}{\mu''}$$

$$-\tfrac{1}{2}e^{-\tau_1/\mu'}\int_0^1 T_1(\tau_1;\mu,\mu'')p^{(0)}(\mu'',-\mu')\frac{d\mu''}{\mu''}, \quad (25)$$

etc.

Using these relations it is possible to make numerical evaluation for successive pairs of T_1, S_1; T_2, S_2; etc.

The emission function $E(\tau_1;\mu)$ is also expanded in a power series of ω, as

$$E(\tau_1;\mu)=\sum_n \omega^n E_n(\tau_1;\mu). \tag{26}$$

Substituting (26) in (21), we have

$$E_0(\tau_1;\mu)=(1-e^{-\tau_1/\mu})(1-\omega)B_\nu(T_c),$$

$$E_1(\tau_1;\mu)=\tfrac{1}{2}(1-\omega)B_\nu(T_c)\int_0^1\{S_1(\tau_1;\mu,\mu')-T_1(\tau_1;\mu,\mu')\}\frac{d\mu'}{\mu'}$$
$$+\frac{1}{2}\int_0^1 p^{(0)}(\mu,\mu')E_0(\tau_1;\mu')d\mu'-\tfrac{1}{2}e^{-\tau_1/\mu}\int_0^1 p^{(0)}(\mu,-\mu')E_0(\tau_1;\mu')d\mu',$$

$$E_2(\tau_1;\mu)=\tfrac{1}{2}(1-\omega)B_\nu(T_c)\int_0^1\{S_2(\tau_1;\mu,\mu')-T_2(\tau_1;\mu,\mu')\}\frac{d\mu'}{\mu'}$$
$$+\frac{1}{4}\int_0^1\int_0^1\{S_1(\tau_1;\mu,\mu')-T_1(\tau_1;\mu,\mu')\}p^{(0)}(\mu',-\mu'')E_0(\tau_1;\mu'')d\mu''\frac{d\mu'}{\mu'}$$
$$+\frac{1}{2}\int_0^1 p^{(0)}(\mu,\mu')E_1(\tau_1;\mu')d\mu'-\tfrac{1}{2}e^{-\tau_1/\mu}\int_0^1 p^{(0)}(\mu,-\mu')E_1(\tau_1;\mu')d\mu'. \tag{27}$$

These expansions in the power of ω correspond to expanding the respective functions by the order of scattering (Goldstein, 1960; Gross, 1962). By use of (24), (25) and (27), $I_{\nu,s}$ and $I_{\nu,e}$ are calculated from (10), (11) and (21) successively as the order of scattering. In evaluating the integrals which appear in (24), (25) and (27), Gauss' quadrature formula is used, where the integrals are divided into 8 for the incident direction and 7 for the scattering direction.

When the air below the cloud is dry, the function $f(\mu)$ in (7) is given by the Plank function for the earth surface temperature, and is isotropic. When it is moist, $f(\mu)$ becomes anisotropic. The calculation of $f(\mu)$ in such a case is well known, and is not repeated here.

5. Results of numerical computation

Numerical computations have been carried out on several model cases with different values of τ_1, T_c and T_s (the earth surface temperature), the combination being listed in Table 1. If we assume the volume concentration of cloud droplets to be 100 cm^{-3}, the optical thickness of $\tau_1=1.0$ corresponds to a geometrical thickness of 89.3 m. This will give the measure of the cloud thicknesses for different τ_1 values and for different volume concentrations.

In all cases listed in Table 1 computations have been made using the boundary condition that $f(\mu)$ is isotropic, i.e., the air below the cloud is dry. As the effect of water vapor in air below the cloud is presumably small, only for the cases with $T_c=-30$ and $T_s=30$ were additional computation made by taking account of anisotropic boundary conditions. In these cases the temperature gradient in the air was assumed to be 5.7C km^{-1}, and the effective amount of water vapor, 3.38 gm cm^{-2}, was assumed to be distributed exponentially with regard to height.

Numerical computation was carried out up to the second power of ω for $\tau_1=0.1$ and 1.0, and to the fourth power of ω for $\tau_1=10$.

The upward intensity at the cloud top. Fig. 3 shows the angular distribution of the upward intensities $I_{\nu,s}$, $I_{\nu,c}$, and $I_\nu(=I_{\nu,s}+I_{\nu,c})$ in the cases with and without the water vapor atmosphere below the cloud and with $\tau_1=0.1$, 1.0, and 10, $T_c=-30$, and $T_s=30$. The ordinate of the figure indicates the intensity in watt m^{-2} sterad^{-1} cm, and the abscissa, the polar angle of the outgoing radiation. The values of the Planck function $B_\nu(T_c)$ and $B_\nu(T_s)$ for $\nu=1000$ cm^{-1}, $T_c=-30$, and $T_s=30$ are indicated on the ordinate as a reference. It will be seen in the figure that in the case of $\tau_1=0.1$ (thin cloud), the total intensity I_ν is mainly due to the transmitted intensity and shows limb darkening. The

TABLE 1. Model cases.

τ_1	0.1	0.1	0.1	0.1	1.0	1.0	1.0	1.0	10	10	10	10
T_c(°C)	−50	−50	−30	−30	−50	−50	−30	−30	−50	−50	−30	−30
T_s(°C)	10	30	10	30	10	30	10	30	10	30	10	30

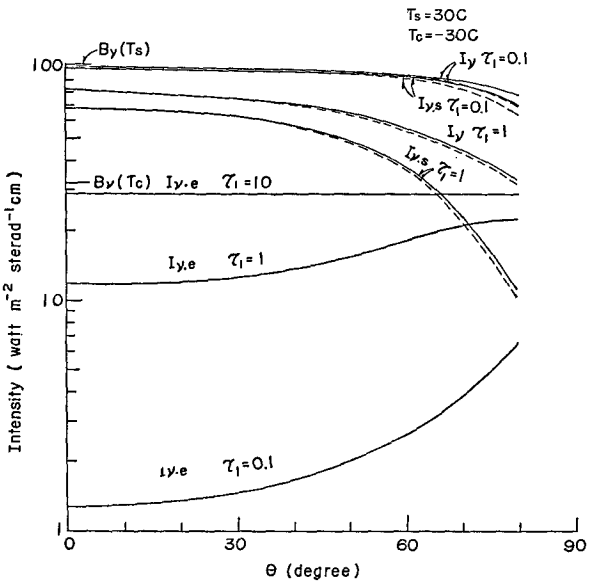

FIG. 3. Angular distribution of the upward intensities $I_{\nu,s}$, $I_{\nu,e}$ and $I_\nu(=I_{\nu,s}+I_{\nu,e})$ at the cloud top for the cases with $T_c=-30$, $T_s=30$ and $\tau_1=0.1$, 1.0 and 10, respectively. Solid lines correspond to the cases with a dry atmosphere below the cloud and broken lines, with a moist atmosphere.

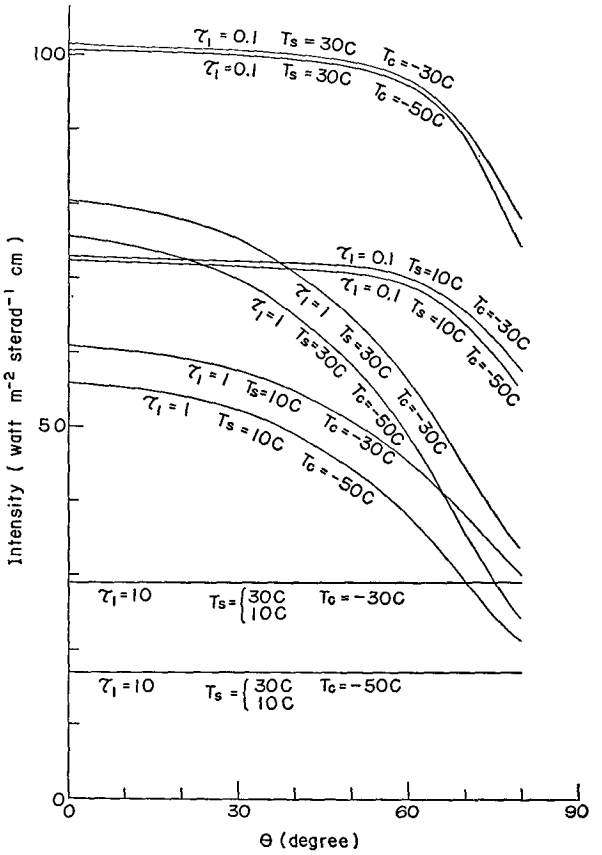

FIG. 4. Angular distribution of the upward intensity I_ν at the cloud top for various cases with a dry atmosphere below the cloud.

emitted intensity is very small and shows limb brightening as it should. In the case of $\tau_1=1.0$ the total intensity and transmitted intensity show more marked limb darkening than for the case of $\tau_1=0.1$. The emitted intensity shows limb brightening as before, and its contribution to the total intensity increases. In the cases of $\tau_1=10$ (thick cloud) the total intensity is primarily due to the emitted intensity and it becomes almost isotropic. The upward intensities in the cases with the water vapor atmosphere below the cloud are shown by the broken lines in the figure. The effect of the water vapor atmosphere slightly increases limb darkening.

The total upward intensity for all the cases listed in Table 1 is shown in Fig. 4. Fig 4 shows that when the cloud is thin ($\tau_1=0.1$) the total upward intensity is mainly dependent on the surface temperature and that when the cloud becomes thick ($\tau_1=10$) it is chiefly determined by the cloud temperature. For clouds of intermediate thickness (for instance $\tau_1=1.0$) it is affected by both the cloud and surface temperatures and limb darkening becomes dominant.

The downward intensity from the cloud base. Fig. 5 shows the angular distribution of the downward intensities in the same cases as shown in Fig. 3. Both $I_{\nu,s}$ and $I_{\nu,e}$ and, accordingly, the total downward intensity I_ν show limb brightening, whose degree decreases with increase of the optical thickness. The contribution of $I_{\nu,e}$ to I_ν is larger than that of $I_{\nu,s}$ regardless of the optical thickness. At the same time the contribution of $I_{\nu,s}$ does not become negligible even for a very thick cloud ($\tau_1=10$).

The total downward intensity in all the cases listed in Table 1 is shown in Fig. 6. It will be seen in the figure that the total downward intensity is mainly dependent on the optical thickness and temperature of the cloud and the effect of the surface temperature is very small.

The flux of radiation in the window region. Information on the transmissivity, reflectivity, and emissivity of the cloud with regard to the flux of radiation in the window region between 8 and 12 microns is very important for various problems of atmospheric radiative transfer. Here, by assuming that the phase function for a wavelength of 10 microns (Fig. 2) can be applicable for the window region, and by using this phase function and the values of ω shown in Fig. 3, the flux of radiation in the window region is calculated. Fig. 7 shows the emissivity, transmissivity, and reflectivity, respectively, of clouds for the window region from 8 to 12 microns, where the emissivity is defined by $\int_{\nu_1}^{\nu_2} F_{\nu,e}d\nu/\pi \int_{\nu_1}^{\nu_2} B_\nu(T_c)d\nu$, the transmissivity by $\int_{\nu_1}^{\nu_2} (F_{\nu,s})_{\tau=0}d\nu/\pi \int_{\nu_1}^{\nu_2} B_\nu(T_s)d\nu$, the reflectivity by $\int_{\nu_1}^{\nu_2} (F_{\nu,s})_{\tau=\tau_1}d\nu/\pi \int_{\nu_1}^{\nu_2} B_\nu(T_s)d\nu$, $F_{\nu,e}$ and $F_{\nu,s}$ are the emitted and scattered flux, respectively, at ν, and ν_1 and ν_2 are the wave numbers corresponding to 12 and 8 microns, respectively. In the figure these quantities are shown as a function of the

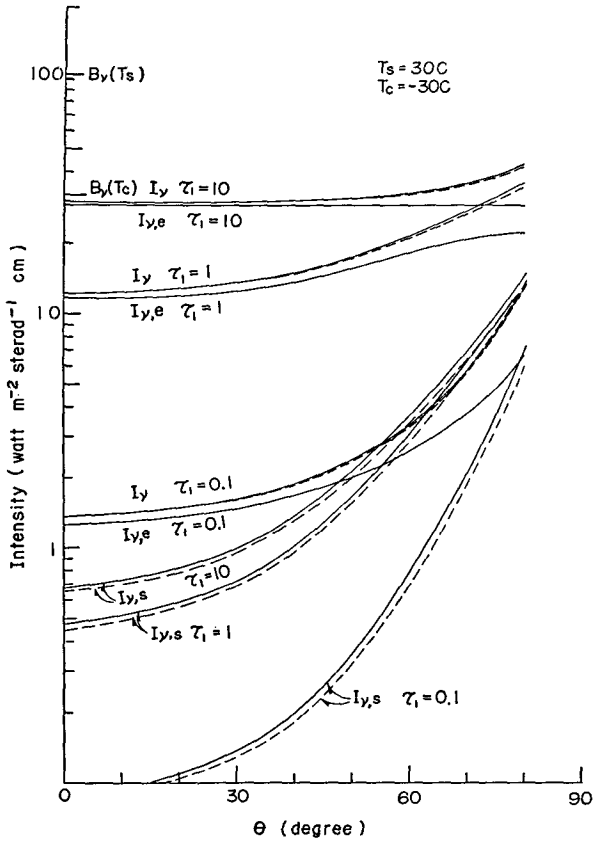

FIG. 5. Angular distribution of the downward intensities $I_{\nu,s}$, $I_{\nu,e}$ and I_ν at the cloud base for the same cases as in Fig. 3.

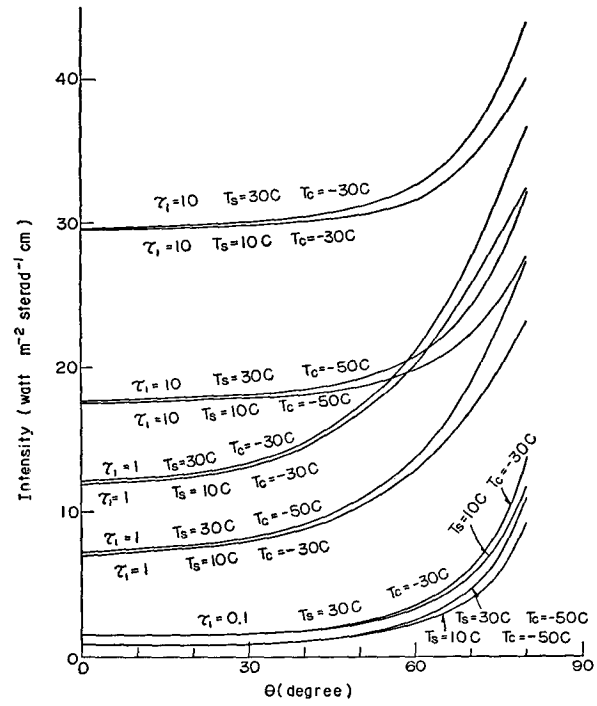

FIG. 6. Angular distribution of the downward intensity I_ν at the cloud base for various cases with a dry atmosphere below the cloud.

number of cloud droplets in a column of 1 cm² cross section which represents the cloud thickness. The optical thickness is not used here, because it changes with wavelength. It will be seen in the figure that the emissivity for the window region increases with increase of the cloud thickness, but is less than one even for the thickest cloud calculated. The reflectivity also increases and asymptotically approaches a constant value with increase of the cloud thickness. On the other hand the transmissivity decreases rapidly with increase of the cloud thickness. According to the definitions of these quantities, it is possible to infer that the emissivity is dependent on the cloud temperature T_c and the transmissivity and reflectivity on the surface temperature T_s. It was found, however, by numerical computation that they are practically independent of temperature, at least for the window region. It will be noticed that by use of the curves in Fig. 7 the upward flux at the cloud top and the downward flux at the cloud base for the window region is easily calculated for various values of T_c, T_s and the cloud thickness.

Fig. 8 shows the upward flux at the cloud top and the downward flux at the cloud base for the cases with $T_c=-50$, $T_s=10$ and $T_c=-30$, $T_s=30$. The figure shows that the relation between the fluxes and cloud thickness is quite similar to that between the intensities and cloud thickness. When the cloud is thin, the upward flux at the cloud top primarily depends on the incident flux corresponding to the earth surface temperature, and when the cloud becomes thick, it approaches blackbody flux at the cloud temperature. The downward flux at the cloud base is very small for a thin cloud, but increases with cloud thickness and approaches a constant value which is somewhat larger

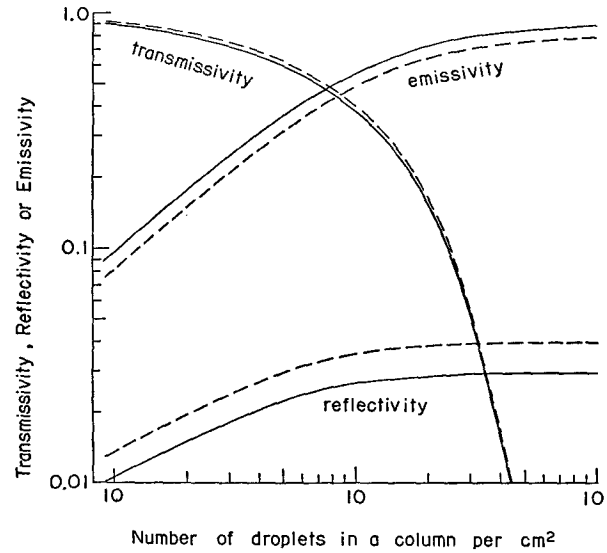

FIG. 7. Emissivity, transmissivity, and reflectivity of clouds for the spectral interval from 8 to 12 microns. Solid lines are due to Deirmendjian's phase function, ω and β_{ext}, and broken lines, due to Deirmendjian's phase function, but with ω and β_{ext} based on Herman's efficiency factor.

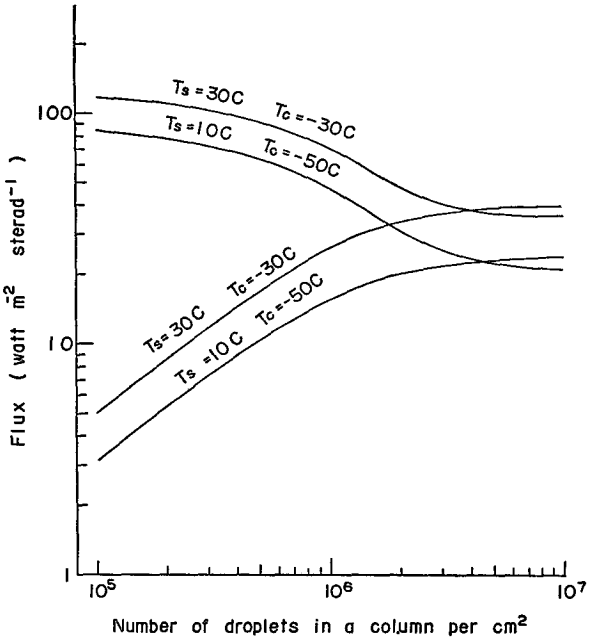

FIG. 8. Upward flux at the cloud top and downward flux at the cloud base for combinations of $T_c=-50$, $T_s=10$ and $T_c=-30$, $T_s=30$.

than the upward flux at the cloud top for the cloud of the same thickness. This is because the reflectivity approaches a constant value for a thick cloud, while the transmissivity becomes negligible. The downward flux which is the sum of the emitted and reflected fluxes, therefore, may theoretically exceed the black body flux at the cloud temperature.

6. Remarks

In this investigation Deirmendjian's values for the phase function and ω are used throughout. However, as discussed in Section 2, the values of ω which are based on Herman's efficiency factor, i.e., on Dorsey's values for the real part and McDonald's values for the imaginary part of the refractive index of water, seem to be more reasonable than those of Centeno's which are adopted by Deirmendjian. Therefore, a supplementary computation of the emissivity, transmissivity, and reflectivity was made using the values of ω and β_{ext} derived from Herman's efficiency factor (Fig. 2) and Deirmendjian's values for the phase function. In Fig. 7 the broken lines indicate the emissivity, transmissivity, and reflectivity due to Herman's values. It will be seen in the figure that the emissivity is less than that of Deirmendjian's, while the transmissivity and reflectivity are larger. The effect of these changes on the upward and downward fluxes is very small when the cloud is thin, but when the cloud becomes thick, both fluxes become less than those based on Deirmendjian's values although the differences are small as expected.

Since the optical properties of water are now fairly well known beyond the window region, it is possible to extend this investigation to the entire infrared region by taking into account the effect of emission and absorption of water vapor in the cloud. Recently Zdunkowski *et al.* (1965) have evaluated the influence of cirrus upon the infrared flux leaving the atmosphere by an approximate method. It would be interesting to investigate radiative transfer in ice clouds based on the phase function for ice crystals.

REFERENCES

Centeno, M., 1941: The refractive index of liquid water in the near infrared spectrum. *J. Opt. Soc. Amer.*, **31**, 244–247.

Chandrasekhar, S., 1950: *Radiative Transfer*. London, Oxford Univ. Press, 393 pp.

Deirmendjian, D., 1964: Scattering and polarization of water clouds and hazes in the visible and infrared. *Appl. Optics*, **3**, 187–196.

Dorsey, N. E., 1940: *Properties of Ordinary Water-Substance*. New York, Reinhold Pub. Co., 673 pp.

Goldstein, J. S., 1960: The infrared reflectivity of a planetary atmosphere. *Astrophys. J.*, **132**, 473–481.

Gross, K. I., 1962: Discussion of an iterative solution to an equation of radiative transfer. *J. Math. Phys.*, **41**, 53–61.

Herman, B. M., 1962: Infrared absorption, scattering and total attenuation cross-section for water spheres. *Quart. J. R. Meteor. Soc.*, **88**, 143–150.

McDonald, J. E., 1960: Absorption of atmospheric radiation by water films and water clouds. *J. Meteor.*, **17**, 232–238.

Plyler, E. K., and N. Acquista, 1954: Infrared absorption of liquid water from 2 to 42 microns. *J. Opt. Soc. Amer.*, **44**, 505.

Wark, D. Q., G. Yamamoto and J. Lienesch, 1962: Infrared flux and surface temperature determinations from TIROS radiometer measurements. Meteorological Satellite Laboratory Report No. 10, U. S. Weather Bureau, 84 pp.

Zdunkowski, W., D. Henderson and J. V. Hales, 1965: The influence of haze on infrared radiation measurements detected by space vehicles. *Tellus*, **17**, 147–165.